

Final Report:

6.2 Terrain Gap Identification and Analysis for Assured Mobility

September 30, 2004

S. Bruce Blundell, Physical Scientist
Verner Guthrie, Physical Scientist
Edmundo Simental, Mathematician



**U.S. Army Engineer Research and Development Center
Topographic Engineering Center
7701 Telegraph Road
Alexandria, VA 22315-3864**

ABSTRACT

Assured land mobility of military forces may be adversely impacted by unexpected discontinuities in terrain that fall within the relative vertical error limits of standard terrain elevation models. We define terrain gaps as consisting of such anomalies, within the context of military maneuver, having characteristic dimensions on the order of ten meters or less and minimum slope of approximately 40 degrees, which may impede or constrain the movement of manned or unmanned ground vehicles. Gaps may be natural or man-made, wet or dry, permanent or transient. They may include irrigation ditches, stream banks, short but steep escarpments, canals, walls, berms, excavation overburden, and other micro-terrain features with a positive or negative elevation difference from immediately surrounding terrain. We examined LIDAR (LIght Detection and Ranging) data over southwestern Montana to capture detailed elevation profiles over suspected terrain gaps, and derived geometric attributes from profile subsets to characterize gap morphology from the perspective of critical military parameters. These data were captured as geospatial information in a GIS environment containing gap linear feature classes with associated attribute data. The profile subsets for each gap feature lend themselves to automatic extraction of elevation breaklines in defining the spatial limits of the gap in the direction of maximum slope change. The distribution of gap features with attribution within the study area demonstrates the critical role that micro-terrain gaps can play in tactical military routing and maneuver models, by obviating bridging, crossing, and avoidance decisions on the ground with advance knowledge of gaps from tactical remote sensors.

Introduction

Terrain elevation modeling and rapid assessment of terrain conditions at relatively high resolutions remains a vital part of tactical military planning for terrain reasoning and mobility corridor determination. A commander must be able to defeat or avoid obstacles at various scales as necessary to achieve success in tactical maneuver operations. Strategies for the defeat of such obstacles include engineering capabilities such as earth-moving systems as well as assault, tactical, and line-of-communications bridging. Avoidance requires advance knowledge of the terrain between the unit's location and the objective. Knowledge about the locations and attributes of obstacles and the ability to disseminate this information directly to commanders in a geospatial context improves situational understanding and decision-making capabilities for ground operations.

From a military perspective, terrain obstacles may be thought of as "gaps" in a commander's ability to achieve operational and tactical maneuver over land. Many of these obstacles manifest themselves as unexpected terrain discontinuities that fall within the relative vertical error limits, or within the horizontal sampling grid, of standard terrain elevation datasets such as U.S. Geological Survey Digital Elevation Models (USGS, 2000). These features may still adversely affect the mobility of manned or unmanned ground vehicles in spite of their limited vertical extent.

Army doctrine for mounted and dismounted maneuver requires the capability to cross water channels and gaps as well as to breach or neutralize obstacles when they cannot be bypassed. The Army's Objective Force must be able to cross narrow gaps such as streams and irrigation ditches without loss of operational momentum (TRADOC, 2003).

For the purposes of this study, we define gaps as micro-terrain features, having characteristic dimensions in the vertical direction on the order of 10 meters or less, with a minimum slope of approximately 45 degrees. Gaps may be natural or man-made, permanent or transient, and in the case of channels or depressions, may contain water on a permanent or intermittent basis. Other micro-terrain features considered to be gaps include ditches, stream banks, escarpments, canals, walls, berms,

excavation overburden, and other small-scale terrain anomalies with a positive or negative elevation difference from immediately surrounding terrain.

In this research, we explore means to identify, geolocate, and characterize gaps, whether natural, man-made, wet, or dry, using a LIDAR (LIght Detection and Ranging) system for high-resolution collection of elevation data. The goal is to assist the commander in assessing locations and characteristics of small-scale terrain gaps that may impede unit mobility. We attach other geometric attributes to each gap, as determined from the LIDAR elevation model, as geospatial information in the ESRI ArcMap environment. Our intent is to develop techniques that will support the generation, management, display, analysis, and distribution of geospatial data for improving gap crossing and avoidance capability for the Army.

LIDAR, an airborne technique for acquiring remotely sensed topographic data, is becoming increasingly important in terrain applications. A LIDAR system is based on sequential range measurements from rapid laser infrared pulses directed toward the ground surface. The ranges are determined from pulse return times back to the sensor. Calculated distances are initially referenced to the survey aircraft, whose position is determined from an on-board Global Positioning System (GPS) receiver. This information is related to a geoid model to provide ground point geographic positions. The pulse sample frequency varies, but common values lie between 1 and 5 meters (Flood and Gutelius, 1997). Typical root mean square error values are 1 to 2 meters for horizontal positions, and 15 to 20 centimeters in the vertical.

Modern LIDAR systems are often able to discriminate the first return, last return, and sometimes multiple returns, from each pulse. First return data represent the first reflective surface, such as a tree canopy, whereas last return data are more likely to represent the ground surface, if the vegetation is not too dense in preventing some laser energy from reaching the ground (Fowler, 2001). With good last return data, coupled with an automatic and/or manual editing process, a Digital Elevation Model (DEM) can be created representing the best estimate of the “bare earth” over the area of LIDAR coverage (Daniel and Tennant, 2001).

Previous Work

The detection of micro-terrain features from elevation models for mobility gap analysis requires sufficient accuracy and sampling resolution that may be provided by airborne remote sensing. Other data types may prove useful in conjunction with high-resolution elevation. Using Ku-band Interferometric Synthetic Aperture Radar (IFSAR) data with 1-meter resolution, Simental and Guthrie (2002) were able to show that minor elevation anomalies were sometimes related to local interferometric decorrelation. Using the same data source, it is possible to identify irrigation ditches of about 1-meter depth in flat agricultural fields through analysis of the IFSAR correlation and elevation files. These features are not always visible on the radar magnitude image (Guthrie and Simental, 2003).

A DEM derived from IFSAR data from TOPSAR, a Jet Propulsion Laboratory/National Aeronautics and Space Administration (JPL/NASA) airborne radar, was employed to identify fault scarps and fault-related lineaments along the Nevada-California border (Hooper, et al., 2003). Extracted profiles revealed that most of the scarps had an average height of over 30 meters, though some detected were as small as 4-6 meters. Other features present in the digital model included benches, levees, cutbanks, and gullies.

For LIDAR data, directed studies have been undertaken to take advantage of the level of vertical accuracy this data provides. These include such applications as river corridor topography (Cobby et al., 2001; Bowen and Waltermire, 2002), coastal elevation changes (Brock et al., 2001; Woolard and Colby, 2002), and local desert topography transformation due to vegetation transitions (Rango, et al., 2000). Yet, due to its highly discrete sampling, LIDAR data are not considered ideal for the detection of elevation breaklines, in spite of the high sampling rate and vertical accuracy. In any digital terrain model, artifacts can occur due to the interpolation scheme employed between points (Florinsky, 2002). The reliability of

slope gradient appears to be more sensitive than slope aspect and form to elevation sampling interval, especially in gently rolling terrain (Gao, 1998). However, for a North Carolina watershed, Hodgson, et al. (2003) found that appreciable terrain slope errors may occur with LIDAR and IFSAR independent of elevation accuracy.

Dataset

The data used in this study consisted of a portion of a LIDAR data collection over southwestern Montana, United States, in the vicinity of the town of Cooke City. The data collection covers an area of 34.8 square kilometers, and was performed as part of the Rapid Terrain Visualization Advanced Concept Technology Demonstration (RTV-ACTD) program, which is managed by the U.S. Army Joint Precision Strike Demonstration Project Office (JPSD-PO). The LIDAR equipment was manufactured by Optech, Inc. and is known as the Airborne Laser Terrain Mapper (ALTM). Normal operating altitudes for such sensors are in the range of 100-2000 meters above the ground (Fowler, 2001). The instrument for the RTV-ACTD program is mounted on a DeHavilland DHC-7 aircraft. After the aircraft's positions during flight are determined with GPS and inertial measurements, the absolute accuracies of each laser pulse are known to within 10-15 centimeters in the vertical and 30-40 centimeters in the horizontal.

The RTV LIDAR co-registered products in the dataset consist of a Digital Elevation Model (DEM) in the form of an elevation image, a color-coded shaded relief image, and an intensity image. The DEM is provided in 32-bit GeoTIFF format with the data output on a grid with a sampling interval of 1-meter. The vertical datum of the DEM is the WGS84 ellipsoid. A conversion factor can be applied to obtain a Mean Sea Level data set if required. The RTV LIDAR instrument can provide both first and last return data; however, only elevation models generated from the last return data were used in this study. The color-coded image is provided in 24-bit color GeoTIFF format and depicts a 1-meter resolution color-mapped shaded relief representation of the elevation model, with the lowest DEM elevations in shades of blue transitioning to shades of red at the higher elevations. The intensity image is an 8-bit grayscale image, also at 1-meter resolution, whose pixels represent the spatially variant reflected intensity of the laser pulse. The GeoTIFF format allows geo-referencing information to be embedded in the file. All image files were transformed into the Universal Transverse Mercator (UTM) projection.

The geology of the Cooke City area is characterized by diverse rock types and mountainous terrain with elevations greater than 2300 meters above sea level. Granites and gneisses underlie much of the area, and numerous wet gaps (streams) and dry gaps exist. Some streams follow joints or cracks in the granitic bedrock. The area is near a complex of ancient volcanoes that produced the debris that covers a significant portion of the region. A series of faults are located to the south and east of Cooke City, and seismic activity has caused uplift of rock slabs. Dikes and sills intrude into metamorphic and sedimentary rocks. Some glacial activity in the area has shaped the hard granite and gneiss landscape into U-shaped valleys. Once the ice melted, overlying conglomerates slumped into these valleys, leaving a scarp-filled, hummocky topography (Alt and Hyndman, 1994; Fritz, 1994). Soda Butte Creek flows through Cooke City and contains substrate materials from granitic gneisses and sedimentary rocks above the town, as well as sediments from volcanics that dominate the northern Yellowstone area (Marcus et al., 2003).

Figure 1 shows the data collection over the study area as represented by the LIDAR color-coded shaded relief image, providing an general overview of the site. North is up in the figure. Longitude extends from 109° 52.7'W to 109° 56.6'W, and latitude from 45° 00.0'N to 45° 03.6'N. Lowest elevations are about 2300 meters in the vicinity of Cooke City with the highest country in the SE corner of the image at about 3000 meters above sea level. The lower half of the image shows heavily wooded high country of the Shoshone National Forest, descending into the Soda Butte Creek valley running east-west through the image. This valley rises to Colter Pass, beyond which lies the valley of Clark's Fork of the Yellowstone River, which flows out of the image on the right.

Figure 2 shows the last return elevation file data over the same area, after a hillshade algorithm was applied to the raw elevation data for each pixel. This representation clearly shows valleys, channels, escarpments, and other features. Elevation differences in the LIDAR pulse response in forested areas due to some of the pulses reaching the ground is represented by fine-grained grayscale variation in the lower and upper portions of the image. The data shown in Figure 2 was used to identify the vertical and horizontal extent of mobility gaps and estimate attributes for slope, natural or man-made origin, and hydrologic state. A portion of this data from the right-center region in a relatively treeless area with discontinuous topography was particularly suitable for the characterization of breaklines. In addition, United States Census TIGER data for roads and hydrologic features represented as linear overlays were used as geo-referenced basemap information in the ArcMap GIS environment.

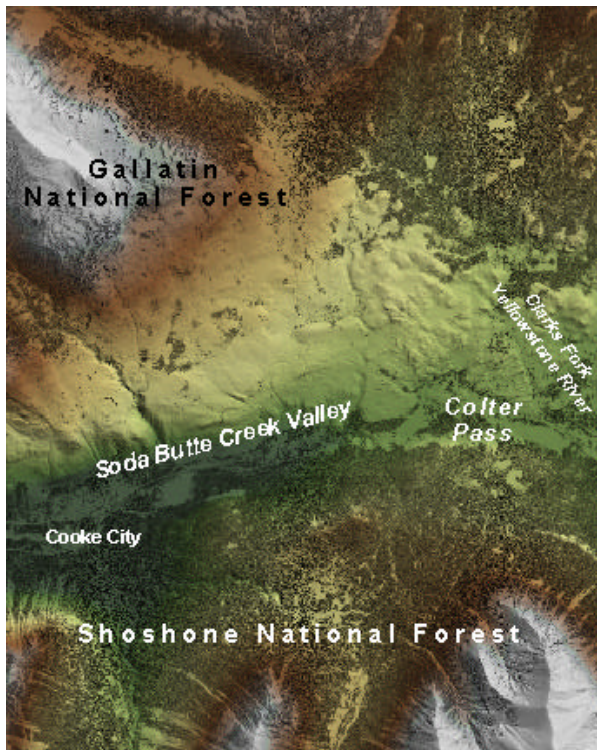


Figure 1. Color-Coded Shaded Relief

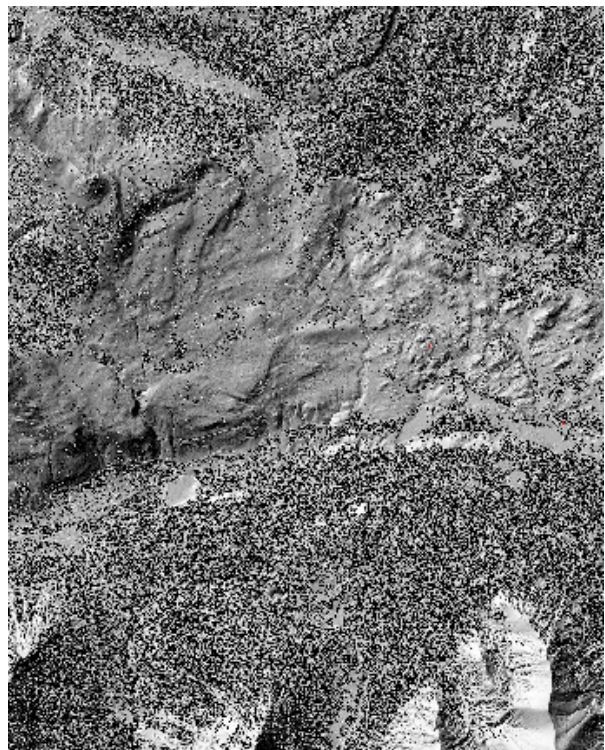


Figure 2. Last Return Elevation Data

Methods

This study involved the display and analysis of a LIDAR elevation model for extraction of micro-terrain breaklines as indicators of mobility gaps, and the collection of geometric attributes through analysis of elevation profiles. The last-return elevation model was used from the RTV LIDAR data files on the assumption that it would provide a greater percentage of pulse returns from the ground surface in forested areas. Bare-earth algorithms are available to semi-automatically remove projections from the model above the ground surface, such as trees and structures. However, we decided to work with original last-return data in order to avoid interpolation of elevation data points, resulting in unrealistic smoothing of actual micro-terrain features. Unwanted anomalies in the model, primarily trees, were recognized as such in the elevation profiles and ignored during attribute collection.

Hillshade and color-coded elevation data were first georeferenced to baseline TIGER vector data representing roads and hydrologic features. The process of gap identification and characterization then commenced, involving the following steps:

- 1) A systematic visual inspection of the hillshade elevation model in ArcMap was conducted, using an overlay grid of 1000 x 1000 meter squares, to identify apparent breaklines that may indicate features that fall under our working definition of gaps as having slopes on the order of 45 degrees or greater, and vertical extent on the order of 10 meters.
- 2) Using the DEM analysis software MICRODEM developed by the Department of Geography and Environmental Engineering at the U.S. Military Academy, a series of elevation profiles was created perpendicular to the linear trend of a suspected gap. If the feature met our minimum gap requirements, it was assigned to a feature class and key geometric characteristics were extracted from the elevation profiles by inspection.
- 3) The gap was entered into an ArcMap layer according to its feature class with its geometry input as attribute information.

The working set of feature classes, feature sub-types, and attributes are given in Table 1. Sub-types and attributes were common to all feature classes.

| Feature Class Layer | Sub-Types | Attributes and Fields |
|-----------------------|----------------|---|
| Channels | <i>Origin:</i> | Length |
| Escarps and Ledges | Man-Made | Maximum Width |
| Depressions and Holes | Natural | Maximum Height |
| Linear Obstructions | Unknown | Maximum Slope |
| Berms or Mounds | | State: Mostly Wet Mostly Dry Perennially Wet/Dry |

Table 1. Feature Class Characteristics

When a suspected gap was identified from the hillshade elevation model, that portion of the model was opened in MICRODEM for quantitative analysis. Figure 3 shows a sub-region of the study area in MICRODEM with overlaid symbology representing elevation profile extractions, from which the feature characteristics in Table 1 were estimated or derived. A sufficient number of elevation profiles were extracted across the length of each feature and in different directions in order to provide a best estimate for the values of maximum width, height, and slope in meters for the vertical obstruction.

The length of each feature was measured as that portion which met the minimum parameters for a gap in height and slope. In the case of a channel, the maximum width and height were measured for one of the side slopes. Maximum slope could be taken from a portion of a slope if the slope varied along the profile. An example of a profile, with no vertical exaggeration, is given in Figure 4. The profile shows a steep escarpment of about 15 meters in height.

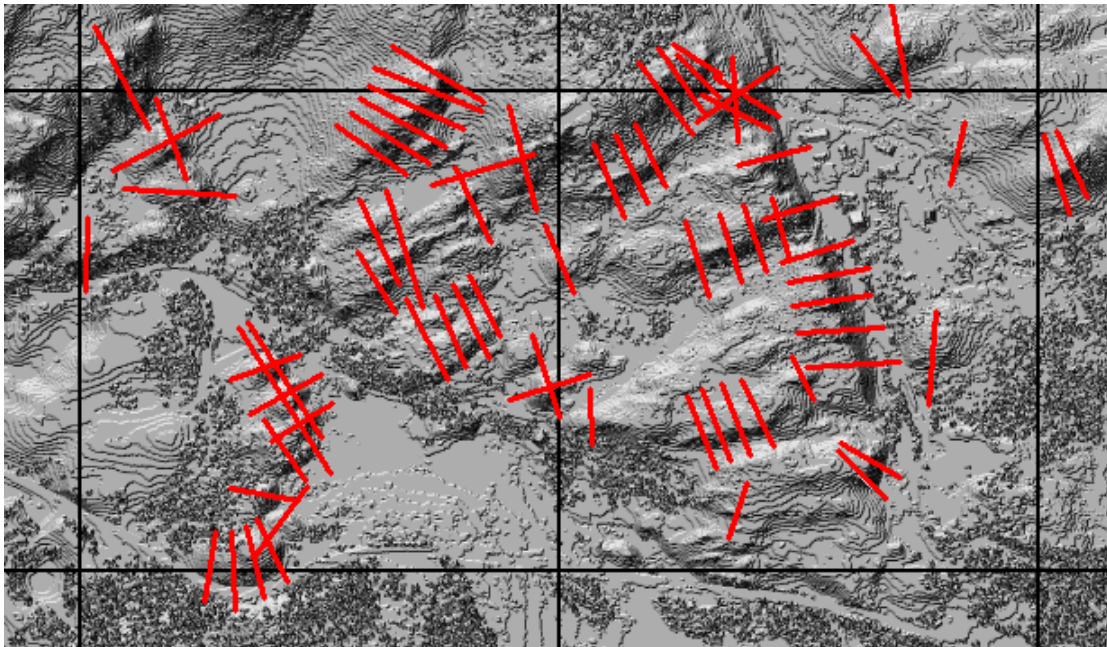


Figure 3. Elevation Profile Extraction Process

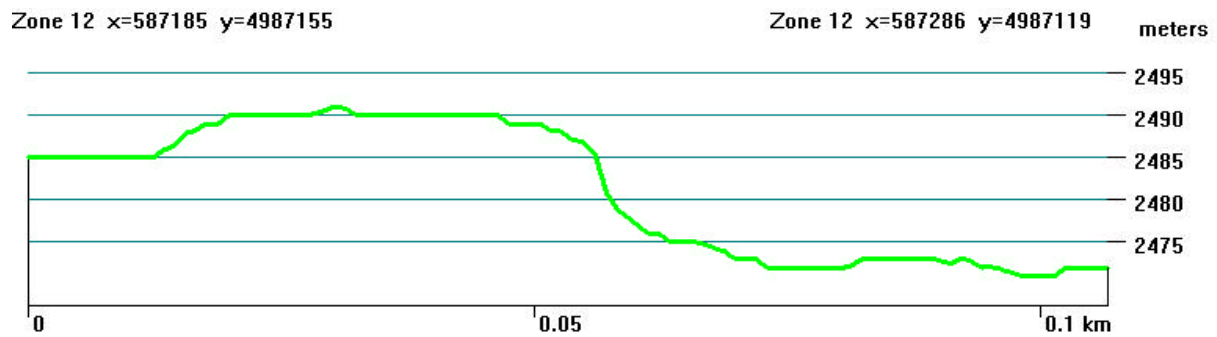











Figure 4. Elevation Profile Example

Results and Discussion

The primary results of this effort were a series of georeferenced ArcMap gap feature overlays with available attribute information. Figure 5 shows a portion of the ArcMap legend with gap features and subtypes organized by color and symbology, alongside an example image of collected features in the area of the town of Cooke City with TIGER surface hydrology and roads data against a color-coded elevation data background. Gap features displayed in this manner with ancillary terrain information can bring added value to mobility planning efforts.

- ☐  **Cooke City Gap Analysis**
 - ☐  HYDRO_tgr
 -
 - ☐  ROADS_tgr
 -
 - ☐  Channel Features
 - Origin
 - Man-made
 - Natural
 - Unknown
 - ☐  Escarpments and Ledges
 - Origin
 - +++ Man-made
 - +++ Natural
 - Unknown
 - ☐  Depressions and Holes
 - Origin
 - +++ Man-made
 - +++ Natural
 - Unknown
 - ☐  Linear Obstructions
 - Origin
 - Man-made
 - Natural
 - Unknown
 - ☐  Berms or Mounds
 - Origin
 - +++ Man-made
 - +++ Natural
 - Unknown
 - ☐  Hillshade of dem_1m_a2_CookeCity_east.tif
 - Value
 - High : 254
 - Low : 0

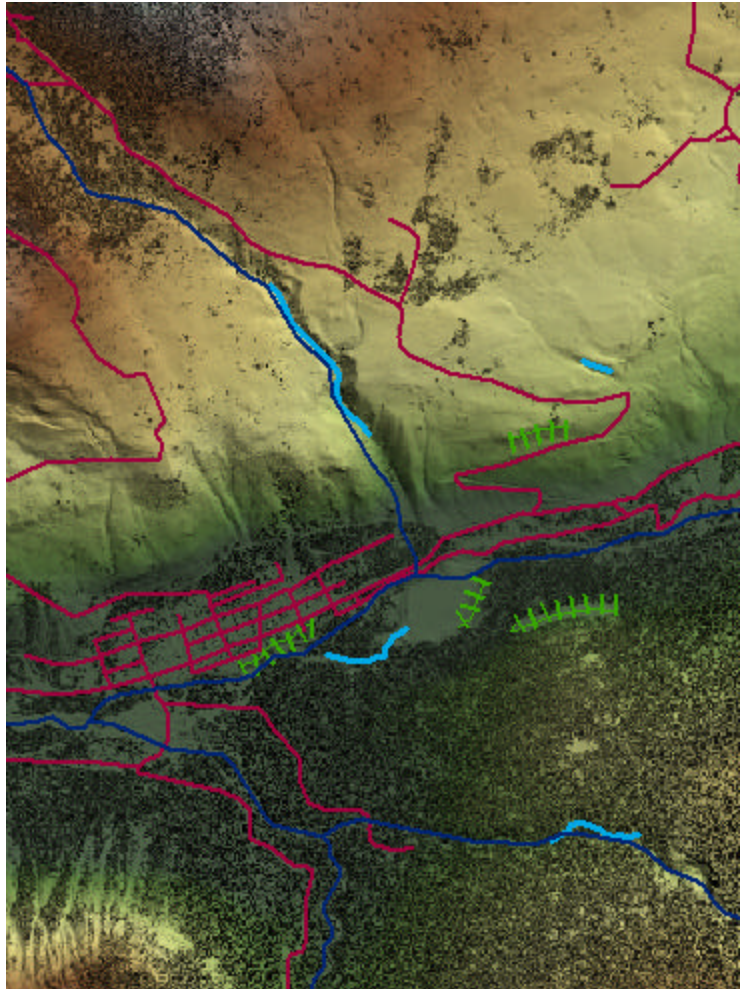


Figure 5. ArcMap Legend with Gap Features Subset

No attempt was made to remove the pulse returns for the tree canopy from the model, in order to preserve the character of breaklines in micro-terrain features. As a result, fewer gaps could be identified under forest, which is itself an impediment to mobility. More gaps could be found in the relatively treeless middle section of the study site, an area of exposed bedrock with discontinuous terrain, many scarps, but fewer stream channels sections whose bank slopes and vertical heights fall within our gap definition parameters.

Table 2 provides some statistics for the geometric parameters of the gap types identified in the study area. Lengths are given in meters. Gap feature types identified in the study area were dominated by escarpments and channels. In comparing channels and escarpments, although the means for maximum height, width, and slope were similar, channel sections showing gap characteristics were, on average, significantly longer than scarps. However, variance among the geometric parameters for both these gap types was high, except in the case of maximum slope. This variance was constrained by the imposed minimum of approximately 40 degrees for inclusion as a gap feature.

| Gap Feature Type | Number of Features | Mean Length | Coeff. Of Variation (%) | Mean Max. Height | Coeff. Of Variation (%) | Mean Max. Width | Coeff. Of Variation (%) | Mean Max. Slope | Coeff. Of Variation (%) |
|------------------|--------------------|-------------|-------------------------|------------------|-------------------------|-----------------|-------------------------|-----------------|-------------------------|
| Escarpments | 40 | 94.7 | 93 | 18.7 | 75 | 24.8 | 100 | 53.4 | 25 |
| Channels | 11 | 206.9 | 89 | 17.5 | 79 | 32.5 | 55 | 49.5 | 31 |
| Berms | 2 | 35.5 | 2.0 | 10.5 | 6.7 | 15.5 | 4.6 | 38.0 | 11.2 |
| Depressions | 1 | 115 | - | 5 | - | 59 | - | 32 | - |

Table 2. Gap Parameter Statistics

In addition to creation of gap feature overlays, we developed an algorithm development strategy for automated gap extraction through analysis of breaklines. Terrain gap anomalies as identified in this study tend to be bounded by slope breaklines that may serve as barriers to mobility. Algorithms may be able to extract breaklines automatically from a LIDAR elevation model and use them to isolate bounded areas containing short, steep slopes. A numerical solution of the function represented by the spatial distribution of elevation values in a matrix would allow estimation of the second derivative of elevation as a breakline indicator. Such an algorithm would find the maximum second derivative and its direction on the horizontal grid for each LIDAR resolution cell. Its sign would then indicate whether the breakline inflection at that point was concave (positive) or convex (negative).

The true form of the spatial distribution of elevation on the horizontal x,y plane $E = f(x,y)$ is unknown and is approximated by the elevation matrix. A second-order, centered finite-divided-difference Taylor series estimation of the slope and Laplacian (second derivative) of the elevation function can be expressed as, respectively,

$$E'_{S,\theta} = (E_{S+2} - 8E_{S+1} + 8E_{S-1} - E_{S-2}) / (12\theta S) \quad (1)$$

and

$$E''_{S,\theta} = (E_{S+2} - 16E_{S+1} + 30E_S - 16E_{S-1} + E_{S-2}) / (12\theta^2 S^2) \quad (2)$$

where E_S is the elevation value at matrix position $S = S(i,j)$ for which the directed slope $E'_{S,\theta}$ and Laplacian $E''_{S,\theta}$ are required in direction θ from position S . θS is the ground distance between adjacent elevation matrix samples in equations (1) and (2) and is a function of θ and the sensor ground sample distance D . Figure 6 depicts an arbitrary LIDAR elevation matrix value S and required matrix value positions at $S+1$ and $S+2$ for calculating $E'_{S,\theta}$ and $E''_{S,\theta}$ in several directions from S . Table 3 gives relative elevation matrix positions for the E terms in (1) and (2), and values for θS , for this series of eight directions from a given matrix location i,j .

This scheme allows for finding the directed derivatives for each matrix position without having to interpolate between matrix values. For eight directions, the minimum value for θS is twice the ground distance, or $2D$. Elevation values are thus taken at every other matrix cell for input into equations (1) and (2). The range of angles is confined to between 0 and 180 degrees. Since the Taylor series estimation is a centered finite-divided-difference formula, derivatives computed for the range 180 to 360 degrees would provide redundant information and are unnecessary.

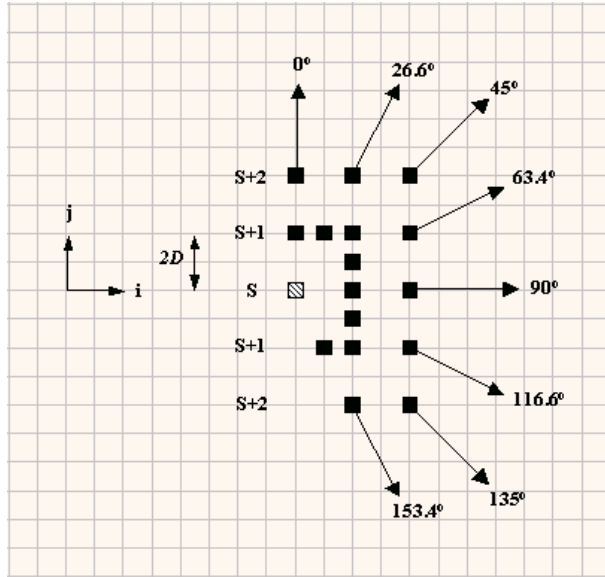


Figure 6. Map of Required Elevation Matrix Elements for Directed Derivative Calculation

| T | S | S+1 | S+2 | S-1 | S-2 | ?S |
|------------------|------|----------|----------|----------|----------|-------------|
| 0^0 | i, j | i, j+2 | i, j+4 | i, j-2 | i, j-4 | $2D$ |
| $\tan^{-1} 1/2$ | i, j | i+1, j+2 | i+2, j+4 | i-1, j-2 | i-2, j-4 | $\sqrt{5}D$ |
| 45^0 | i, j | i+2, j+2 | i+4, j+4 | i-2, j-2 | i-4, j-4 | $\sqrt{8}D$ |
| $\tan^{-1} 2$ | i, j | i+2, j+1 | i+4, j+2 | i-2, j-1 | i-4, j-2 | $\sqrt{5}D$ |
| 90^0 | i, j | i+2, j | i+4, j | i-2, j | i-4, j | $2D$ |
| $\tan^{-1} -1/2$ | i, j | i+2, j-1 | i+4, j-2 | i-2, j+1 | i-4, j+2 | $\sqrt{5}D$ |
| 135^0 | i, j | i+2, j-2 | i+4, j-4 | i-2, j+2 | i-4, j+4 | $\sqrt{8}D$ |
| $\tan^{-1} -2$ | i, j | i+1, j-2 | i+2, j-4 | i-1, j+2 | i-2, j+4 | $\sqrt{5}D$ |

Table 3. Relative Elevation Matrix Positions and ?S Values for Eight Directions

For each matrix position, the direction of maximum Laplacian is found. The end result of the process is a set of parameters associated with each matrix cell in addition to elevation: maximum slope, maximum Laplacian, sign of inflection (convex/concave), and direction. Potential breaklines could be formed connecting points with Laplacian magnitude values above a given threshold, whose relative directions lie within given constraints, under the assumption that breaklines change direction gradually over short distances. Gaps may then be identified as regions with slopes above a threshold, adjoining a breakline or bounded by close, parallel breaklines. Sets of matrix points forming breaklines, or regions of steep slopes associated with breaklines, could then be incorporated into a GIS environment as gap features, with key geometric parameters as attribute information.

Summary and Conclusions

The increased resolution and accuracy of elevation data from modern LIDAR systems are proving useful in a variety of earth resource applications. From a military perspective, traditional sources of elevation models such as 30 meter DEMs are often inadequate for assured mobility in tactical settings. This problem must be solved in order to meet the requirement for mobile units to defeat micro-terrain gaps by crossing or avoidance. Advance knowledge of the type, location, and characteristics of gaps available in a geographic information system can be a useful tool for cross-country planning purposes. Fine-grained terrain information will be even more critical for the smaller wheelbases of future unmanned ground vehicles.

If slope breaklines can be considered useful indicators of the spatial limits of gap features, the refinement of numerical algorithms for finding breaklines from high-resolution terrain models will increase the speed and accuracy of gap identification. Slope breakline information may then be processed and organized into individual linear gap features as geo-located objects in a GIS, whose extent would be constrained by input geometric parameters. In spite of the difficulty of discovering breaklines using a discrete sampling scheme, current and future LIDAR sensors may provide adequate resolution for characterizing micro-terrain anomalies from an elevation model.

Future work may include development and testing of effective breakline-finding algorithms, based on the algorithm development strategy described above. Such work would include the determination of algorithm constraints and thresholds under field conditions. We also intend to experiment with “bare-earth” LIDAR elevation models to reduce the capture of spurious breaklines resulting from neighboring pulse returns from tree canopies and adjacent terrain. Additional work is possible in the investigation of elevation models derived from Interferometric Synthetic Aperture Radar (IFSAR) over the same site for comparative analysis with the LIDAR data in modeling micro-terrain discontinuities. In addition to modeling mobility barriers, such efforts would complement studies of the geomorphic distribution of fault scarps. To date, the results from this preliminary study indicate that high-resolution elevation models show strong potential for the extraction of specialized slope/terrain products, with the promise of more efficient capture of these features by semi-automated and automated means.

Acknowledgments

The authors wish to thank Steven Sarigianis, U.S. Army Joint Precision Strike Demonstration Project Office (JPSD-PO) for providing the Rapid Terrain Visualization LIDAR data, with the assistance of Mary Brenke and Peggy Diego, U.S. Army Engineer Research and Development Center, Topographic Engineering Center (ERDC-TEC) Imagery Office. Nathan Campeau (ERDC-TEC Operations Division) provided invaluable assistance with geodatabase creation in ArcMap. Melody Clanton (ERDC-TEC Management Information Office) and Rebecca Ragon (ERDC-TEC Research Division) provided graphic support.

REFERENCES

- Alt, D. and D. Hyndman (1994). *Roadside Geology of Montana*. Mountain Press Publishing Company, Missoula, Montana.
- Bowen, Z.H. and R.G. Waltermire (2002). Evaluation of light detection and ranging (LIDAR) for measuring river corridor topography. *Journal of the American Water Resources Association* 38(1):33-41.

- Brock, J.C., C.W. Wright, A.H. Sallenger, W.B. Krabill and R.N. Swift (2001). Recognition of fiducial surfaces in lidar surveys of coastal topography. *Photogrammetric Engineering and Remote Sensing* 67(11):1245-1258.
- Cobby, D.M., D.C. Mason and I.J. Davenport (2001). Image processing of airborne scanning laser altimetry data for improved river flood modelling. *ISPRS Journal of Photogrammetry and Remote Sensing* 56:121-138.
- Daniel, C. and K. Tennant (2001). DEM quality assessment. In: *Digital Elevation Model Technologies and Applications: The DEM Users Manual*. American Society for Photogrammetry and Remote Sensing, Bethesda, MD-USA, pp. 395-440.
- Flood, M. and B. Gutelius (1997). Commercial implications of topographic terrain mapping using scanning airborne laser radar. *Photogrammetric Engineering and Remote Sensing* 63:327-329,363-366.
- Florinsky, I.V. (2002). Errors of signal processing in digital terrain modelling. *International Journal of Geographical Information Science* 16(5):475-501.
- Fowler, R. (2001). Topographic lidar. In: *Digital Elevation Model Technologies and Applications: The DEM Users Manual*. American Society for Photogrammetry and Remote Sensing, Bethesda, MD-USA, pp. 207-236.
- Fritz, W.J. (1994). *Roadside Geology of the Yellowstone Country*. Mountain Press Publishing Company, Missoula, Montana.
- Gao, J. (1998). Impact of sampling intervals on the reliability of topographic variables mapped from grid DEMs at a micro-scale. *International Journal of Geographic Information Systems* 12(8):875-890.
- Guthrie, V. and E. Simental (2003). Detecting micro-terrain features using high resolution interferometric synthetic aperture radar (IFSAR). *Proceedings of the American Society for Photogrammetry and Remote Sensing (ASPRS), Anchorage, Alaska, May 2003*.
- Hodgson, M.E., S. Schill, B. Davis, J.R. Jensen and L. Schmidt (2003). An evaluation of LIDAR- and IFSAR-derived digital elevation models in leaf-on conditions with USGS level 1 and level 2 DEMs. *Remote Sensing of Environment* 84(2):295-308.
- Hooper, D.M., M.I. Bursik and F.H. Webb (2003). Application of high-resolution, interferometric DEMs to geomorphic studies of fault scarps, Fish Lake Valley, Nevada-California, USA. *Remote Sensing of Environment* 84(2):255-267.
- Marcus, W.A., C.J. Legleiter, R.J. Aspinall, J.W. Boardman and R.L. Crabtree (2003). High spatial resolution hyperspectral mapping of in-stream habitats, depths, and woody debris in mountain streams. *Geomorphology* 55:363-380.
- Rango, A., K. Havstad, W. Kustas, T. Schmutge, M. Chopping and J. Ritchie (2000). Morphological characteristics of shrub coppice dunes in desert grasslands of southern New Mexico derived from scanning LIDAR. *Remote Sensing of Environment* 74(1):26-44.
- Simental, E. and V. Guthrie (2002). Application of the interferometric synthetic aperture radar (IFSAR) correlation file for use in feature extraction. *Proceedings of the International Society for Optical Engineering (SPIE), Seattle, Washington, July 2002*.
- TRADOC (2003). *Military Operations – Force Operating Capabilities*. TRADOC Pamphlet 525-66, Department of the Army Training and Doctrine Command, Fort Monroe, Virginia, 30 January 2003.
- USGS (2000). *US GeoData Digital Elevation Models*. Fact Sheet 040-00 (April 2000), United States Geological Survey (USGS), Department of the Interior, Washington, DC.
- Woolard, J.W. and J.D. Colby (2002). Spatial characterization, spatial resolution, and volumetric change of coastal dunes using airborne LIDAR: Cape Hatteras, North Carolina. *Geomorphology* 48:269-287.